JACS
JOURNAL OF THE AMERICAN CHEMICAL SOCIETY
Article
pubs.acs.org/JACS

Singlet Oxygen-Engaged Selective Photo-Oxidation over Pt Nanocrystals/Porphyrinic MOF: The Roles of Photothermal Effect and Pt Electronic State

Yu-Zhen Chen,[†] Zhiyong U. Wang,[‡] Hengwei Wang,[†] Junling Lu,[†] Shu-Hong Yu,[†] and Hai-Long Jiang*[,†]

[†]Hefei National Laboratory for Physical Sciences at the Microscale, CAS Key Laboratory of Soft Matter Chemistry, Collaborative Innovation Center of Suzhou Nano Science and Technology, School of Chemistry and Materials Science, University of Science and Technology of China, Hefei, Anhui 230026, People's Republic of China

[‡]Department of Chemistry and Physics, Troy University, Troy, Alabama 36082, United States

Supporting Information

ABSTRACT: The selectivity control toward aldehyde in the aromatic alcohol oxidation remains a grand challenge using molecular oxygen under mild conditions. In this work, we designed and synthesized Pt/PCN-224(M) composites by integration of Pt nanocrystals and porphyrinic metal−organic frameworks (MOFs), PCN-224(M). The composites exhibit excellent catalytic performance in the photo-oxidation of aromatic alcohols by 1 atm O_2 at ambient temperature, based on a synergetic photothermal effect and singlet oxygen production. Additionally, in opposition to the function of the Schottky junction, injection of hot electrons from plasmonic Pt into PCN-224(M) would lower the electron density of the Pt surface, which thus is tailorable for the optimized catalytic performance via the competition between the Schottky junction and the plasmonic effect by altering the light intensity. To the best of our knowledge, this is not only an unprecedented report on singlet oxygen-engaged selective oxidation of aromatic alcohols to aldehydes but also the first report on photothermal effect of MOFs.

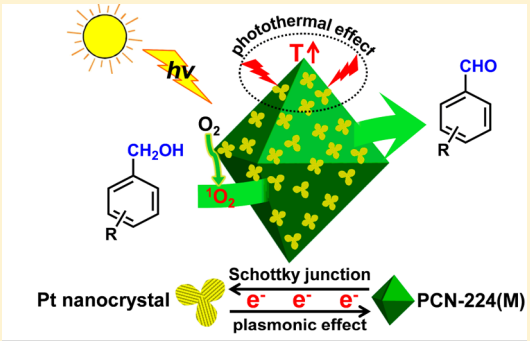

INTRODUCTION

Selective oxidation of primary alcohols to aldehydes is an important laboratory and commercial procedure for the production of fine chemicals and intermediates.[1−8] While the reaction can be traditionally effected with stoichiometric inorganic and organic oxidants, there have been ongoing active efforts to develop new catalytic systems using environmentally benign reagents such as molecular oxygen.[9,10] In this regard noble metal nanoparticles (NPs) such as Au NPs supported on metal oxides have been developed as effective catalysts,[4−8] although there are still limitations including low selectivity and harsh reaction conditions requiring high temperature or high pressure, organic solvents, strong oxidants, or corrosive environment. Molecular oxygen in its ground state exists in the triplet state ($^3\Sigma_g^-$), and upon activation it can be turned into two singlet excited states, $^1\Delta_g$ and $^1\Sigma_g$, 95 and 158 kJ/mol above the triplet state, respectively.[11] Singlet oxygen ($^1O_2$), a mild yet efficient oxidant, has proven to be a versatile reactive oxygen species with applications in multiple organic transformations as well as photodynamic cancer therapy,[12−21] but so far it has not been applied to the oxidation of aromatic alcohols.[22,23] It is assumed that the $^1O_2$ species might be effective in the oxidation of alcohols, and its moderate oxidation ability will merit the selectivity to aldehydes against over-oxidation, although this remains unexplored thus far. In this context, the development of efficient photosensitizers and catalysts, which are critical for both $^1O_2$ production and the selective alcohol oxidation under mild conditions, is highly desirable.

Various photosensitizers, such as metal NPs, porphyrins, and their derivatives, have been reported to effectively generate $^1O_2$.[22−27] We reason that the integration of the photosensitizers into porous materials, such as metal−organic frameworks (MOFs),[28−31] could result in their synergistic and superior functions. MOFs have captured widespread interest and found applications in many diverse fields in the recent two decades due to their high surface area and great structural tailorability.[32−52] Recently, porphyrinic MOFs have been reported to be effective photosensitizers for $^1O_2$ generation and exhibit good catalytic activity for oxidation reactions using $^1O_2$ as an oxidant.[16−18] On the other hand, Pt-group metal nanocrystals (NCs) can not only activate O_2 to $^1O_2$ under light irradiation but also adsorb and activate alcohols in catalytic oxidation of alcohols.[6,9,26,53,54] Moreover, the photothermal effect converting light into heat has been recently realized on

Received: November 23, 2016
Published: January 20, 2017

DOI: 10.1021/jacs.6b12074
J. Am. Chem. Soc. 2017, 139, 2035−2044

metal NCs based on localized surface plasmon resonance (LSPR) and been shown to promote the reactivity of metal NCs.[49,55−58] With these facts, Pt NCs could be a promising catalyst for oxidation of alcohols with O_2 under light irradiation. The optimized electronic state of Pt surface, similar to that of Pd,[13] is critical for O_2 activation and oxidation reactions, for which the formation of heterojunction structure of metal/semiconductor is an effective approach.[59−63] Therefore, the integration of Pt NCs with semiconductor-like porphyrinic MOFs as $^1O_2$ generator could achieve their synergistic effects and provide optimized Pt electronic state and an efficient catalytic system for alcohol oxidation.

On the basis of the aforementioned considerations, we have rationally set out to stabilize Pt NCs by porphyrinic MOFs, namely, PCN-224(M) (M represents the metal ion residing in the center of porphyrin ligand),[34] to afford composite catalysts, Pt/PCN-224(M). The optimized Pt/PCN-224(Zn) composite combines the advantages of both Pt NCs and PCN-224(Zn), lying in their photothermal effect and $^1O_2$ production ability, and exhibits excellent catalytic activity and selectivity in the oxidation of primary alcohols to aldehydes via a singlet oxygen-engaged oxidation process by using O_2 under very mild conditions involving visible-light irradiation (Scheme 1). To the best of our knowledge, this is the first report on the singlet oxygen-engaged oxidation of aromatic alcohols and also the first finding of a photothermal effect by MOFs.

Scheme 1. Schematic Illustration Showing the Singlet Oxygen-Engaged Selective Oxidation of Alcohols over Pt/PCN-224(M) Using Molecular Oxygen under Visible-Light Irradiation

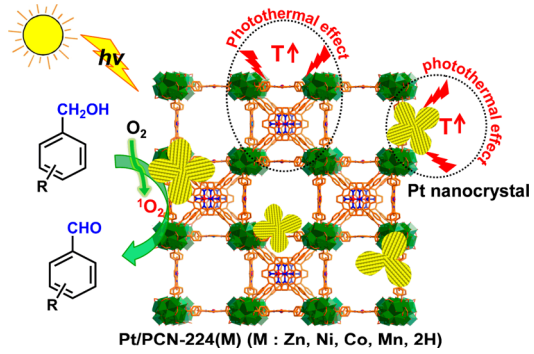

MATERIALS AND METHODS

Materials and Equipment. All chemicals were from commercial suppliers without further purification unless otherwise mentioned. Powder X-ray diffraction (XRD) patterns were measured on a Japan Rigaku SmartLab rotation anode X-ray diffractometer or Holland X'Pert PRO fixed anode X-ray diffractometer equipped with graphite monochromatized Cu Kα radiation (λ = 1.54178 Å). The UV−vis absorption spectra were recorded on a UV−vis spectrophotometer (UV-2700, Shimadzu) in the wavelength range of 200−800 nm. The content (6.3 wt %) of Pt in Pt/PCN-224(Zn) was quantified by an Optima 7300 DV inductively coupled plasma atomic emission spectrometer (ICP-AES). The size, morphology, and microstructure of Pt/PCN-224(Zn) were investigated by transmission electron microscopy (TEM) on a JEOL-2010 with an electron acceleration energy of 200 kV and scanning electron microscopy (SEM, Zeiss Supra 40 scanning electron microscope at an acceleration voltage of 5 kV). The X-ray photoelectron spectroscopy (XPS) measurements were conducted by using an ESCALAB 250 high-performance electron spectrometer using monochromated Al Kα radiation ($h\nu$ = 1486.7 eV) as the excitation source. Nitrogen sorption isotherms were measured by an automatic volumetric adsorption equipment (Micromeritics, ASAP 2020). Prior to nitrogen adsorption/desorption measurements, the as-synthesized samples were activated in DMF and acetone and then dried in vacuum at 60 °C. Following that the product was dried again by using the "outgas" function for 12 h at 80 °C. Electron spin resonance spectra (ESR) were recorded on JES-FA200 electron paramagnetic resonance spectrometer under visible-light irradiation (λ > 400 nm). Catalytic oxidation reaction products were analyzed and identified by gas chromatography (GC, Shimadzu 2010 Plus with a 0.25 mm × 30 m Rtx-5 capillary column). GC-MS analysis was performed on an Agilent Technologies 7890B GC system equipped with an Agilent Technologies 5977B MSD Mass Spectrometer. The metal dispersion was measured by CO chemisorption using a fully automated chemisorption analyzer (Micromeritics, Autochem II 2920) at 323 K. Prior to CO titration, the catalysts were treated at 423 K for 60 min under a hydrogen gas flow and then cooled to 323 K under a helium gas atmosphere. The metal dispersion was calculated assuming a stoichiometry of one CO molecule per surface metal atom.

Preparation of Ligand. The tetrakis(4-carboxyphenyl)porphyrin (TCPP) and other metal-involved TCPP (M-TCPP) ligands were synthesized based on previous reports with minor modifications.[34]

Preparation of PCN-224(M) (M: Zn, Ni, Co, Mn, and 2H). PCN-224(M) were prepared based on the reported procedure with minor modifications.[34] For PCN-224(M) (M = Zn, Co, and 2H): typically, $ZrCl_4$ (120 mg), Zn−TCPP or Co−TCPP or H_2TCPP (40 mg), benzoic acid (1.2 g), and 0.5 mL of acetic acid in 7.5 mL of DMF were ultrasonically dissolved in a 20 mL Teflon-lined autoclave and heated in a 120 °C oven for 24 h. For PCN-224(Ni), $ZrCl_4$ (40 mg), Ni−TCPP (40 mg), benzoic acid (1.0 g), and 0.5 mL of acetic acid in 7.5 mL of DMF were ultrasonically dissolved in a 20 mL Teflon-lined autoclave and heated in a 120 °C oven for 24 h. For PCN-224(Mn), $ZrCl_4$ (40 mg), Mn−TCPP (40 mg), benzoic acid (1.8 g), and 0.5 mL of acetic acid in 7.5 mL of DMF were ultrasonically dissolved in a 20 mL Teflon-lined autoclave and heated in 120 °C oven for 24 h. For all samples, dark brown crystals were harvested by filtration and washing.

Preparation of ZIF-8. The synthesis of ZIF-8 powder was based on a previous procedure with some modifications.[64] Typically, $Zn(NO_3)_2{\cdot}6H_2O$ (1.68 g) was dissolved in 80 mL of methanol, followed by a mixture of 2-methylimidazole (3.70 g) with 80 mL of methanol being added into the above solution with vigorous stirring for 24 h. The white product was separated by centrifugation, washed thoroughly with methanol, and finally dried for 12 h at 50 °C. The ZIF-8 powder was further activated at 200 °C under vacuum prior to use.

Preparation of Branched Pt nanocrystals (~10 nm). The branched Pt nanocrystals (NCs) in good dispersion were prepared according to a reported procedure with modifications.[65] Typically, a volume of 2.5 mL of ethylene glycol (EG) was preheated at 120 °C for 10 min. Then 94 μL of 0.375 M polyvinylpyrrolidone (PVP, MW = 55 000) and 47 μL of 0.0625 M $H_2PtCl_6{\cdot}6H_2O$ aqueous solution were added to the EG every 30 s over a 16 min period with constant vigorous stirring (total volumes for PVP and $H_2PtCl_6{\cdot}6H_2O$ solutions are 3 and 1.5 mL, respectively). The resulting mixture was kept at 120 °C for an additional 10 min and then cooled down to room temperature. The product was centrifuged at 14 000 rpm for 5 min and washed thoroughly with water several times to remove excess PVP. The precipitate was collected and redispersed in water to obtain an aqueous solution of Pt NCs (2 mg/mL) with a size of ~10 nm.

Preparation of Pt/PCN-224(M) and Pt/ZIF-8 Composites. The Pt/PCN-224(M) or Pt/ZIF-8 composites were prepared by introducing as-synthesized MOF into the synthetic system of Pt NCs (0.0256 mmol). Typically, the mixture of PCN-224(M) or ZIF-8 (50 mg) in ethylene glycol (EG, 2.5 mL) was ultrasonically dispersed and then preheated at 120 °C for 10 min. Following that 94 μL of 0.375 M polyvinylpyrrolidone (PVP, MW = 55 000) and 47 μL of 17 mM $H_2PtCl_6{\cdot}6H_2O$ aqueous solution was added to the EG every 30 s over a 16 min period with constant vigorous stirring (total volumes for PVP and $H_2PtCl_6{\cdot}6H_2O$ solutions are 3 and 1.5 mL, respectively). The resulting mixture was kept at 120 °C for an additional 10 min and then

DOI: 10.1021/jacs.6b12074
J. Am. Chem. Soc. 2017, 139, 2035−2044

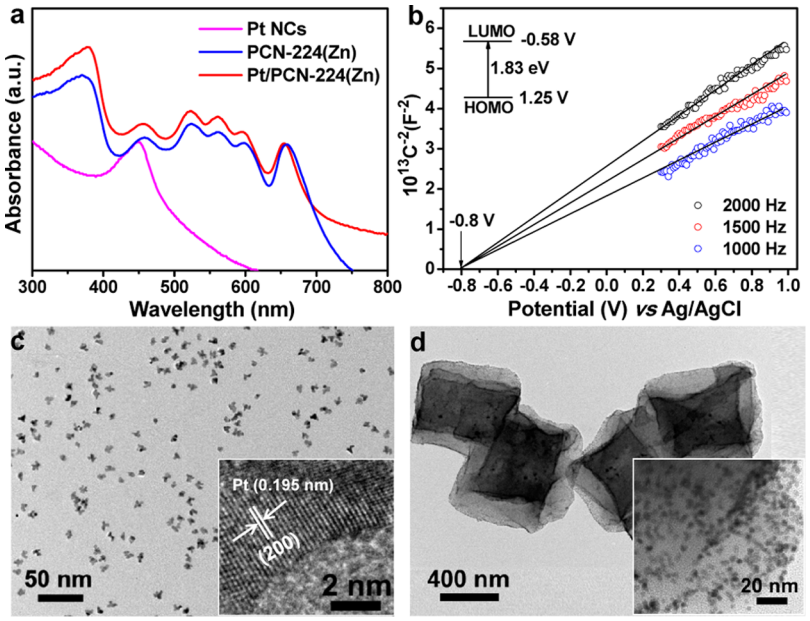

Figure 1. (a) UV−vis spectra of PCN-224(Zn), Pt NCs, and Pt/PCN-224(Zn). (b) Mott−Schottky plots for PCN-224(Zn) in 0.2 M Na_2SO_4 aqueous solution (pH 6.8); (inset) energy diagram of the HOMO and LUMO levels of PCN-224(Zn). (c) TEM and HRTEM (inset) images for Pt NCs. (d) TEM and enlarged TEM images for Pt/PCN-224(Zn).

cooled down to room temperature. The obtained product was collected by centrifugation and washed thoroughly several times with water and ethanol. The synthesized sample was further dried overnight at 323 K under dynamic vacuum for further use. The PVP concentration was changed to 1.125 M for synthesis of ∼2.5 nm Pt NCs, and no PVP was added for ∼14 nm Pt NCs, while other parameters were fixed.

Preparation of Pd Octahedron Nanocrystals (∼15 nm). The Pd octahedron nanocrystals were prepared according to a reported procedure.[66] Typically, 0.105 g of PVP, 0.060 g of citric acid, and 0.060 g of L-ascorbic acid were dissolved in 8 mL of deionized water in a 3-neck flask. The mixture was heated in air at 120 °C for 5 min. The Pd stock solution (0.065 g of K_2PdCl_4 in 3 mL of deionized water) was then added dropwise into the flask within 30 min. The reaction was kept at 120 °C in air for 3 h. The precipitate was washed with acetone and then with ethanol thoroughly to remove the PVP and other molecules by centrifugation.

Photocurrent Measurement. Photocurrent measurements were performed on a workstation (Chenhua Instrument, Shanghai, China) in a standard three-electrode system with the photocatalyst-coated FTO as the working electrode, Pt plate as the counter electrode, and Ag/AgCl as the reference electrode. A 300 W xenon lamp with a visible-light cutoff filter (>400 nm) was used as the light source. A 0.2 M Na_2SO_4 electrolyte was bubbled with nitrogen for 20 min before the measurements. The as-synthesized Pt NCs, PCN-224(Zn), and Pt/PCN-224(Zn) composites (5 mg) were added into 2 μL of Nafion and 1 mL of ethanol mixed solution, and the working electrodes were prepared by dropping the suspension (100 μL) onto the surface of a FTO plate. The working electrodes were dried at room temperature, and the photoresponsive signals of the samples were measured under chopped light at 0.6 V.

Mott−Schottky Plot Measurement. Mott−Schottky plots of PCN-224(Zn) were measured on a electrochemical workstation (Zahner Zennium) in a standard three-electrode system with the photocatalyst-coated electrode as the working electrode, Pt plate as the counter electrode, and Ag/AgCl as the reference electrode at frequencies of 1000, 1500, and 2000 Hz, respectively. A 0.5 M Na_2SO_4 solution deoxygenated using N_2 stream was used as the electrolyte. The preparation procedure of the working electrode is similar to that for the photocurrent measurement described above.

3,3′,5,5′-Tetramethylbenzidine (TMB) Oxidation. TMB (5 mg) was mixed with 3 mL of HAc/NaAc buffer solution (0.2 M: 0.2 M) and 1 mL of H_2O. Then an aqueous suspension of 100 μL of PCN-224(Zn) (3.2 mg/mL), 10 μL of Pt nanocrystals (2 mg/mL), or 100 μL of Pt/PCN-224(Zn) (3.2 mg/mL) was added into the reaction mixture with O_2 bubbling at 20 °C under visible-light irradiation. The concentration of Pt NCs was kept the same as that in Pt/PCN-224(Zn). The samples were taken at different time intervals for UV−vis measurements. The measurements were also performed under other gas environments (N_2 and air). To verify the type of active oxygen species, different scavenger molecules were added into the solution prior to the UV−vis measurements: (1) carotene (10 mg); (2) mannite (2 mg); (3) catalase (200 unit/mL, 2 mg); (4) superoxide dismutase (SOD, 1350 unit/mL, 500 μL).

2,2,6,6-Tetramethyl-4-piperidone Hydrochloride (4-oxo-TMP) Oxidation and ESR Analysis. A 10 μL amount of an aqueous suspension of PCN-224(Zn) (3.2 mg/mL), 1 μL of an aqueous suspension of Pt nanocrystals (2 mg/mL), or 10 μL of an aqueous suspension of Pt/PCN-224(Zn) (3.2 mg/mL) was mixed with 500 μL of 4-oxo-TMP solution (50 mM). The measurements were conducted at room temperature under incident light irradiation with USHIO Optical Modulex SX-U1501XQ (500 W, λ > 400 nm) or in the dark.

Confirmation Experiments for Singlet Oxygen Production. Some classical probe molecules, such as 1,3-diphenylisobenzofuran (DPBF),[16] 9,10-dimethylanthracene (DMA),[67] singlet oxygen sensor green (SOSG, Molecular Probe),[68] and terpene hydrocarbons (α-terpinene),[69] have been used to detect singlet oxygen. The test based on DPBF was carried out using a visible-light source at room temperature. Typically, 10 mg of DPBF was dissolved in 4 mL of DMF with 10 μL of an aqueous suspension of Pt/PCN-224(Zn) (3.2 mg/mL). The stock solutions of fluorescent DMA or SOSG were prepared by dissolving 6 mg of DMA in 6 mL of dimethylformamide or 100 μg of SOSG in 1 mL of methanol. Then 2 μL of the sensor solution was mixed with 3 mL of D_2O with or without 10 μL of aqueous suspension of Pt/PCN-224(Zn) (3.2 mg/mL).

5,5-Dimethyl-1-pyrroline *N*-Oxide (DMPO) Ring-Opening Reaction and Corresponding ESR Analysis. A 10 μL amount of an aqueous suspension of Pt/PCN-224(Zn) (3.2 mg/mL) was mixed with 0.5 mL of water. Then 20 μL of DMPO was added into the solution. The measurements were conducted at room temperature under incident light irradiation with USHIO Optical Modulex SX-U1501XQ (500 W, λ > 400 nm).

Alcohol Oxidation Reactions Conducted at Ambient Temperature. In general, a mixture of 1.25 mg of Pt NCs or 20

DOI: 10.1021/jacs.6b12074
J. Am. Chem. Soc. 2017, 139, 2035−2044

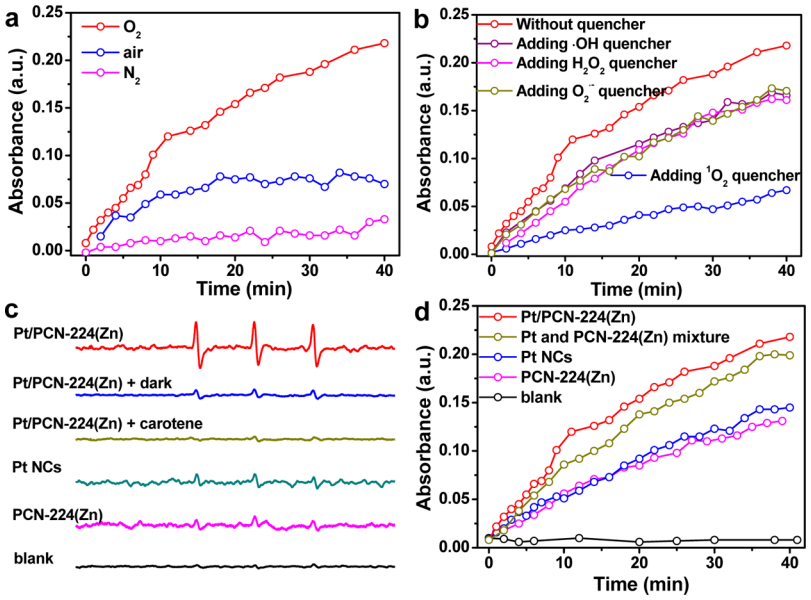

Figure 2. UV−vis peak intensity for the TMB oxidation product vs reaction time (a) over Pt/PCN-224(Zn) in various gas environments, (b) over Pt/PCN-224(Zn) in the presence of different scavengers, and (d) over different catalysts in bubbled O_2. (c) ESR spectra of the samples after mixing 4-oxo-TMP solution with PCN-224(Zn), Pt NCs, and Pt/PCN-224(Zn) in the absence or presence of carotene under visible-light irradiation or in dark. A curve for the 4-oxo-TMP solution was collected as the reference.

mg of 6.3 wt % Pt/PCN-224(Zn) (determined by ICP analysis) or PCN-224(M), 20 μmol of alcohol compounds (or toluene), and 10 mL water was placed in a three-neck flask (25 mL). The catalytic oxidation reaction was initiated at ambient temperature (~16 °C) with 1 atm O_2 under visible-light irradiation with a 300 W Xe lamp (λ > 400 nm, PLS-SXE300, Beijing Perfectlight Technology Co., LTD, China). The solution temperature of the reaction system was monitored throughout the reaction. After the reaction, the catalyst was separated by centrifugation, thoroughly washed with water and ethanol, and then reused in subsequent runs. The yield of the product was analyzed by GC with *n*-dodecane as the internal standard. For comparison, 20 mg of Pt/ZIF-8 as a catalyst was examined for the reaction, while all other reaction parameters and processes were kept the same. For the testing of the oxidation ability of H_2O_2 for benzyl alcohol, 1.25 mg of Pt NCs, 1 mL of H_2O_2, 9 mL of H_2O, and 20 μmol of benzyl alcohol were mixed in the absence of light irradiation.

Alcohol Oxidation Reactions Conducted at a Fixed Temperature (T = 16 °C). In general, a mixture of 20 mg of 6.3 wt % Pt/PCN-224(M) or PCN-224(M), 20 μmol of alcohol, and 10 mL of water was placed in a photocatalytic reactor. The temperature of the mixture solution was fixed at 16 °C by flowing condensate water. The catalytic oxidation reaction was carried out in the presence of 1 atm O_2 under visible-light irradiation with a 300 W Xe lamp (λ > 400 nm). The yield of the product was analyzed by GC with *n*-dodecane as the internal standard.

Alcohol Oxidation Reaction over Pd Octahedron Nanocrystals. In general, a mixture of 2.5 mg of Pd octahedra, 20 μmol of benzyl alcohol, and 10 mL of water was placed in a three-neck flask (25 mL). The catalytic oxidation reaction was conducted at 80 °C or ambient temperature with 1 atm O_2 in the absence of visible-light irradiation.

RESULTS AND DISCUSSION

A series of chemically stable PCN-224(M) (M = Zn, Ni, Co, Mn, 2H) were obtained via solvothermal reactions at 120 °C according to a previous procedure (Figure S1).[34] Their structures contain both channels and cages with sizes as large as ~19 Å (Figure S2). The N_2 sorption experiment on the representative PCN-224(Zn) indicates high porosity and a large BET surface area of 2018 m^2/g (Figure S3). The UV−vis spectrum of PCN-224(Zn) shows strong adsorption in the range of 300−800 nm (Figure 1a), revealing the photon absorption and electron−hole separation ability upon visible-light irradiation. The positive slopes of Mott−Schottky plots for PCN-224(Zn) at frequencies of 1000, 1500, and 2000 Hz are consistent with the behavior of a typical *n*-type semiconductor (Figure 1b). The flat band position (LUMO) determined from the intersection is ca. −0.80 V vs Ag/AgCl or −0.58 V vs normal hydrogen electrode (NHE). The valence band (HOMO) is then calculated to be 1.25 V vs NHE, considering that the band gap energy of PCN-224(Zn) is estimated to be 1.83 V from the Tauc plot (Figure S4).

Pt NCs were obtained by reacting $H_2PtCl_6{\cdot}6H_2O$ in ethylene glycol (EG)/H_2O in the presence of polyvinylpyrrolidone (PVP) at 120 °C for 10 min.[65] Transmission electron microscopy (TEM) and high-resolution TEM (HRTEM) images clearly show the branched Pt NCs in tripod or tetrapod shape with good dispersion, uniform size (~10 nm), and great crystallinity (Figures 1c and S5a). The broad adsorption of Pt NCs in the UV−vis spectrum indicates the SPR property (Figure 1a). The Pt/PCN-224(M) composite was assembled by preaddition of PCN-224(M) into the synthetic system of Pt NCs. The crystallinity and structure of PCN-224(M) are well maintained upon combination with Pt NCs (Figure S1). The slight decrease of surface area in reference to parent PCN-224(Zn) is ascribed to the mass occupation of Pt NCs (Figure S3). Scanning electron microscopy (SEM) shows that PCN-224(Zn) has a uniform size (~800 nm) and is mostly in an octahedral shape (Figure S5b), and Pt NCs are uniformly dispersed on the surface of PCN-224(Zn) in the composite (Figures 1d and S5c,d).

O_2 activation is a key step in the O_2-involved oxidation reactions. To examine the ability of Pt/PCN-224(M) composites for O_2 activation, TMB was employed as the initial model compound to undergo oxidation over Pt/PCN-224(Zn) as a representative. Upon oxidation by different active oxygen species, the colorless TMB was changed to two colored products with characteristic UV−vis peaks at 370 and 652 nm

DOI: 10.1021/jacs.6b12074
J. Am. Chem. Soc. 2017, 139, 2035−2044

(partially oxidized product I, blue) as well as 450 nm (fully oxidized product II, yellow) (Figure S6).[70] Interestingly, TMB molecules were mainly oxidized into partially oxidized intermediate by Pt NCs, PCN-224(Zn), and Pt/PCN-224(Zn) composite (Figure S6), revealing their moderate oxidation power, which is essential for selective oxidation of primary alcohols into aldehydes but not carboxylic acids. This result prompted us to compare the oxidation of benzyl alcohol with O_2 by Pt/PCN-224(Zn) versus $KMnO_4$. While excellent selectivity for benzaldehyde was achieved with Pt/PCN-224(Zn), the stronger oxidant $KMnO_4$ gave benzoic acid as a main product (Figure S7).

The dramatically different oxidation rates for TMB in various gas environments (N_2, O_2, and air) suggest that an active oxidative species is indeed evolved from O_2 (Figures 2a and S8). To clarify which active oxygen species is actually generated in our system, various scavengers including carotene, mannite, catalase, and superoxide dismutase (SOD) were introduced into the reaction system to specifically inhibit the generation of $^1O_2$, $^\bullet OH$, H_2O_2, and $O_2^{\bullet-}$, respectively.[71] As shown in Figure 2b, only carotene significantly suppresses the oxidation of TMB, indicating that the main active species generated by Pt/PCN-224(Zn) composite is $^1O_2$. The fact that oxidation is not completely inhibited by carotene suggests that some minor oxidation pathways other than $^1O_2$ oxidation might be also in effect. Furthermore, 4-oxo-TMP, a well-known probe molecule for $^1O_2$ due to its ability to trap $^1O_2$ to afford the stable nitroxide radical 4-oxo-TEMPO, further confirms the $^1O_2$ generation through electron spin resonance (ESR) measurement. ESR spectra display a 1:1:1 triplet with a g value of 2.030 characteristic of signals of 4-oxo-TEMPO for all samples (Figure 2c),[72] demonstrating the formation of $^1O_2$ or at least a species that displays chemical properties of $^1O_2$. Among Pt/PCN-224(Zn), its two components, and the simple physical mixture of two components, Pt/PCN-224(Zn) exhibits the strongest UV absorbance for TMB oxidation product (Figure 2d) and the strongest signals of 4-oxo-TEMPO (Figure 2c), confirming the synergy between Pt NCs and the MOF for $^1O_2$ production.[16,26] The signals are almost completely quenched by carotene or in the dark (Figure 2c), again manifesting that they are originated from $^1O_2$ indeed and light is necessary for $^1O_2$ generation. To further confirm the generation of $^1O_2$ based on Pt/PCN-224(Zn) by light irradiation, a variety of classical $^1O_2$ probe molecules including DPBF, DMA, and SOSG have been examined. All obtained results corroborate each other and reveal that an active $^1O_2$ species is indeed formed in our reaction system (Figures S9–11).

Since oxidative species other than $^1O_2$ could be responsible for our observed reactions, we checked whether any of them is formed in a significant amount. The radical trapping agent DMPO is particularly useful for identifying $O_2^{\bullet-}$ and $^\bullet OH$. The ESR spectra display a 1:1:1 triplet signal consistent with DMPO/$^1O_2$. Neither the 1:1:1:1 quartet signal from DMPO/$^\bullet O_2H$ nor the 1:2:2:1 quartet signal from DMPO/$^\bullet OH$ was detected (Figure S12), disqualifying radicals as responsible oxidants in our reaction system.[73] α-Terpinene is an excellent probe compound for our system because it will be converted to ascaridole with $^1O_2$ but to other aromatic products with $O_2^{\bullet-}$ and $^\bullet OOH$.[69] Ascaridole was detected as the nearly exclusive product after 4 h in our reaction conditions, again corroborating $^1O_2$ engagement (Figure S13). Our proposed mechanism is consistent with the generation of $^1O_2$ but inhibited conversion of O_2 to $O_2^{\bullet-}$ based on PCN-224(Zn) upon light irradiation (Scheme S1).

With the above information in hands, we are in a position to investigate the photo-oxidation of aromatic alcohols by O_2 over Pt/PCN-224(M) or related catalysts under visible-light irradiation. The reaction has been conducted with benzyl alcohol in water with 1 atm O_2 at ambient temperature (16 °C). The data for catalytic oxidation of benzyl alcohol in Table 1 indicates that Pt/PCN-224(Zn) exhibits the highest catalytic activity among all catalysts with 100% selectivity for aldehyde production, and the reaction is complete in 50 min (entry 1). The reaction does not produce benzoic acid even if it is extended to longer reaction time, manifesting the superb selectivity of catalyst (entry 1). On the basis of the 3.4% of accessible Pt sites from a CO titration experiment (Figure S14), the turnover frequency (TOF) is calculated to be as high as 269 h^{-1}. Under identical conditions, only 56% of benzyl alcohol is oxidized over Pt NCs after 60 min, and negligible activity can be detected with PCN-224(Zn) (entries 2 and 3), suggesting that alcohols can be activated on the Pt surface while the MOF

Table 1. Oxidation of Benzyl Alcohol by O_2 over Different Catalysts under Visible-Light Irradiation Started from Ambient Temperature (16 °C)[a]

entry	catalyst	time	T (°C)	yield[b] (%)
1	Pt/PCN-224(Zn)	30 min	34	84
		50 min	36	>99
		12 h	36	>99
2	Pt NCs	30 min	26	39
		60 min	28	56
3	PCN-224(Zn)	30 min	26	5
		60 min	28	5
4	Pt + PCN-224(Zn)	30 min	28	37
		60 min	28	62
5[c]	Pt/PCN-224(Zn)	30 min	16	52
		60 min	16	86
6	Pt/PCN-224(Ni)	30 min	27	59
		60 min	27	97
7	Pt/PCN-224(Co)	30 min	30	52
		60 min	28	83
8	Pt/PCN-224(Mn)	30 min	28	61
		60 min	28	81
9	Pt/PCN-224	30 min	30	41
		60 min	30	62
10	Pt/ZIF-8	60 min	26	52
11	Pt/PCN-224(Zn)	30 min	16–35[d]	35
12[e]	Pd NCs	60 min	80	>99
13[f]	Pt NCs	120 min	25	23
14	Pt/PCN-224(Zn) + carotene	30 min	34	15
		60 min	36	31
15[g]	Pt/PCN-224(Zn)	12 h	38	>99

[a]Reaction conditions: catalyst (20 mg, 6.3 μmol Pt), alcohol (20 μmol), 10 mL of H_2O, visible light (λ > 400 nm, 100 mW/cm^2), O_2 (1 atm). [b]Yield of aldehyde was analyzed by GC, and n-dodecane was used as the internal standard. [c]At a fixed reaction temperature of 16 °C. [d]The reaction was from 16 to 35 °C within 30 min by external heating in the absence of light irradiation, with the heating speed similar to that by photothermal effect. [e]Pd NCs (2.5 mg), 80 °C, in the absence of light. [f]H_2O_2 (1 mL), H_2O (9 mL), alcohol (20 μmol), without O_2 bubbling and visible-light irradiation. [g]Alcohol (1 mmol), catalyst (31.5 μmol of Pt).

DOI: 10.1021/jacs.6b12074
J. Am. Chem. Soc. 2017, 139, 2035–2044

has no such ability.[9] The mere 62% yield for the physical mixture of Pt NCs and PCN-224(Zn) (entry 4), significantly lower than that of the composite, should be ascribed to the absence of interaction between separated Pt NCs and the MOF.

An unusual photothermal effect has been observed for the reaction. Upon visible-light irradiation for 30 min, the reaction temperature spontaneously increases from 16 to 26 °C for both Pt NCs and PCN-224(M) and 36 °C for Pt/PCN-224(Zn), evidently higher than the resulting temperature (18 °C) of the reaction system in the absence of catalyst or the presence of ZIF-8 (Table S1). Both Pt NCs and PCN-224(M) obviously have a photothemal effect, which is synergistically enhanced in Pt/PCN-224(M). We propose that the visible-light-responsive porphyrin unit in PCN-224(M) is responsible for converting the light to heat, as other nonporphyrin-based MOFs like ZIF-8 cannot. To the best of our knowledge, neither the photothermal effect of MOFs nor the synergistic photothermy between Pt NCs and MOFs has been reported previously.

The synergistic photothemal conversion of Pt/PCN-224(Zn) is an important finding as photoinduced heat is highly desirable for endothermal reactions. When the reaction temperature was fixed at 16 °C to eliminate photoinduced heat, only 52% and 86% yields can be obtained for Pt/PCN-224(Zn) after 30 and 60 min, respectively (Table 1, entry 5, and Figure 3). Pt/ZIF-8 gave a similar activity to Pt NCs (entries 2 and 10), mainly because ZIF-8 cannot convert light into heat. It is noteworthy that the catalytic activities of Pt/PCN-224(M) composites increase with more d electrons of central metals (no metal, Mn, Co, Ni, Zn) in the porphyrin (entries 1 and 6–9). To exclude the influence of a photothermal effect, reactions with different catalysts were conducted under identical conditions at a fixed temperature (16 °C), and the same activity order was observed (Table S2). It is assumed that the d electron number of the metal centered in the metalloporphyrin in MOFs influences the triplet states of porphyrin, which play important roles in both the activation ability of triplet O_2 (Scheme S2) and possibly the energy transfer between MOF and Pt,[19,22] reasonably explaining the distinct activity in Pt/PCN-224(M).

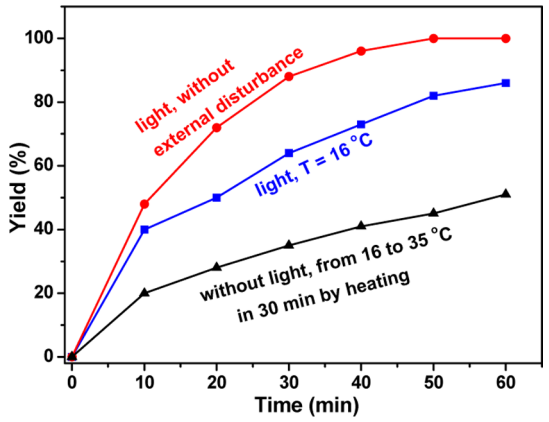

Figure 3. Oxidation yield of benzyl alcohol vs reaction time over Pt/PCN-224(Zn) in the presence or absence of light irradiation or external heating, while other reaction parameters were kept unchanged.

To assess the importance of light, the catalytic oxidation over Pt/PCN-224(Zn) was carried out with all parameters unaltered except changing light irradiation to heating, in which the yield was only 35% after 30 min, far below that under visible-light irradiation (entry 11 and Figure 3).

All experimental evidence points to the conclusion that $^1O_2$ or some other species from it is responsible for our observed alcohol oxidation, which was rarely reported.[13,22,23] Pd octahedron nanocrystals was reported to generate $^1O_2$ solely and oxidize glucose.[13] We synthesized Pd NCs according to literature procedures and applied it to benzyl alcohol oxidation (Figure S15). The reaction achieved complete conversion to benzaldehyde after 1 h at 80 °C in water (entry 12). More importantly, when the reaction was performed at ambient temperature, 35% conversion to benzaldehyde was achieved after 12 h (data not shown). This is clear that $^1O_2$ is engaging the selective oxidation of alcohol to aldehyde, albeit in low efficiency with Pd NCs. Moreover, ESR analysis of the radical trapping agent DMPO excludes the formation of the radicals (e.g., $O_2^{\bullet-}$ and $^{\bullet}OH$), as indicated above (Figure S12). Another possible oxidant that could be formed in our reaction system is hydrogen peroxide. However, direct introduction of H_2O_2 into the benzyl oxidation reaction to replace $^1O_2$ results in much lower activity, indicating that H_2O_2 is not the responsible oxidant in our reaction system (entry 13). To further exclude the formation of other reactive oxygen species (ROS) and/or conversion of $^1O_2$ into other ROS in the reaction system, four specific scavengers that exclusively inhibit the generation of $^1O_2$, $^{\bullet}OH$, H_2O_2, and $O_2^{\bullet-}$ species, respectively, were introduced into the reaction system in varying amounts. While the reaction yield quickly decreased with increasing amounts of the $^1O_2$ quencher carotene (only 31% yield was obtained even after 60 min by adding 20 mg of $^1O_2$ quencher; entry 14), it showed no response to varying amounts of other quenchers even at ~2 orders of magnitude of theoretically consumed amount (Figure S17). These results unambiguously rule out the other three types of ROS and demonstrate the involvement of $^1O_2$ from O_2 activation by Pt/PCN-224(M) in the reaction of benzyl alcohol. The above evidence collectively supports that $^1O_2$ is indeed generated (see SI, section 4) and is truly engaged and responsible in our benzyl alcohol oxidation system. We proposed a tentative reaction pathway (Scheme S3). However, the exact mechanism, including the specific roles played by $^1O_2$ to boost the reaction, remains to be clarified by more experiments and/or theoretical calculations. Since $^1O_2$ alone is inefficient at oxidizing benzyl alcohol, we propose that visible light, photothermal effect, $^1O_2$, and the diamagnetism of metal ion residing in porphyrin center synergistically contribute to the excellent activity and selectivity in the oxidation of benzyl alcohol to benzaldehyde using O_2 over the Pt/PCN-224(M) composite.

In consideration of the potential for practical applications, the reaction with increased amount of substrate was also conducted (entry 15). With 1 mmol (~0.10 g) of alcohol the reaction took longer time (12 h) to finish, but it is remarkable that exclusive and quantitative formation of benzaldehyde is still achieved without external heat input. Noteworthily, in addition to the representative Pt/PCN-224(Zn) with ~9 nm Pt NCs described above, the Pt/PCN-224(Zn) with Pt NCs of ~3 and ~14 nm have been synthesized (Figure S16), and they also present 100% selectivity toward benzaldehyde, though lower activity compared to that with ~9 nm Pt NCs, in the oxidation of benzyl alcohol under identical reaction conditions (Table S3).

DOI: 10.1021/jacs.6b12074
J. Am. Chem. Soc. 2017, 139, 2035–2044

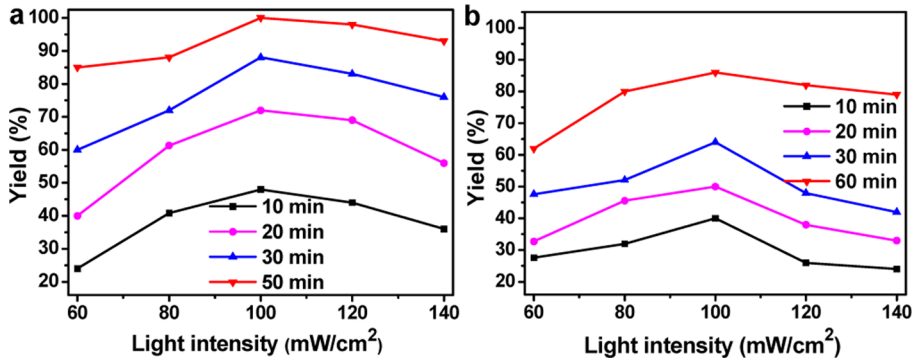

Figure 4. Oxidation yield of benzyl alcohol over Pt/PCN-224(Zn) at different light intensities under visible-light irradiation at (a) spontaneous reaction temperatures and (b) a fixed reaction temperature (16 °C).

To further understand the role of visible light and the interaction between Pt and PCN-224(M), the catalytic performance of Pt/PCN-224(Zn) as a representative has been investigated for benzyl alcohol oxidation under varying light intensities (60−140 mW/cm^2, λ > 400 nm). The reaction yields increase with enhanced light intensity from 60 to 100 mW/cm^2 and then decrease when the light intensity is further increased (Figure 4a). The positive relationship between reaction yields and light intensity in the range of 60−100 mW/cm^2 can be explained by a photothermal effect, as stronger light intensity leads to a higher reaction temperature, which is favorable for the endothermic process (Figure S18 and Table S4). The drop of reaction yield after the light intensity further increases beyond 100 mW/cm^2, however, indicates that other factors also control the reaction. Reactions were thus conducted at a constant temperature (16 °C) to exclude the photothermal effect, and a similar correlation between reaction yield and light intensity was observed (Figure 4b). The results imply the presence of electron transfer between Pt NCs and PCN-224(Zn) under light irradiation, and thus, the electron density of the Pt surface changes along with light intensity. It has been reported that O_2 activation and oxidation reaction are positively correlated with the electron density on the surface of Pd-group metals.[62] Meanwhile, the modulation of the charge state of the active metal surface has been well documented in the noble metal/semiconductor (M−S) hybrid configuration based on electron transfer via the Schottky junction and/or plasmonic effect.[59−63] In our system, both Pt NCs and PCN-224(Zn) are able to accept photons of visible light and can be excited to produce photoelectrons. Upon visible-light irradiation with relatively low intensity (<100 mW/cm^2), PCN-224(Zn) is readily photoexcited and electron−hole pairs are separated. The electrons on the conductive band (LUMO) of PCN-224(Zn), with the behavior of an *n*-type semiconductor, flow to the Fermi level of Pt, promoted by the presence of a Schottky junction. Higher light intensity would induce the delivery of more electrons to the Pt surface, making it more electron rich, which is beneficial to the activation of O_2 to $^1O_2$ and thus improves the catalytic activity.[62] When the light intensity further increases (>100 mW/cm^2), the hot electrons of Pt NCs can be generated by the excitation of surface plasmons (plasmonic effect), which is more competitive than a Schottky junction for electron transfer between Pt NCs and PCN-224(Zn). As a result, the electrons from Pt NCs are injected into the conductive band (LUMO) of PCN-224(Zn), producing the electron-deficient surface of Pt sites, which is disadvantageous to $^1O_2$ generation and lowers catalytic activity.[62] The above results indicate that the electronic density of the Pt surface can be flexibly regulated by adjusting light intensity, which holds the key to modulation of $^1O_2$ generation and the catalytic activity of alcohol oxidation (Scheme S4; Section 5).

This electron transfer between Pt NCs and PCN-224(Zn) was further studied by transient photocurrent measurement for PCN-224(Zn), Pt NCs, and Pt/PCN-224(Zn) (Figure S19). While the current density of separate PCN-224(Zn) or Pt NCs stays positively correlated with light intensity from 60 to 120 mW/cm^2, the current density of Pt/PCN-224(Zn) composite initially increases with increasing light intensity up to 100 mW/cm^2 and then subsequently decreases when light intensity is further increased. The results corroborate with the trend observed for reaction yield vs light intensity and indicate improved charge separation in Pt/PCN-224(Zn) driven by the Schottky barrier at a relatively low light intensity (<100 mW/cm^2) and the reverse injection of energetic hot electrons from the plasmonic Pt NCs to reach the M−S interface and enter the LUMO of PCN-224(Zn) at high light intensity (>100 mW/cm^2). The flow of electrons in Pt/PCN-224(Zn) composite at different light intensities is very consistent with the catalytic results, and the mechanism is illustrated in Scheme 2.

The recycling stability of a heterogeneous catalyst is of great importance for its practical application. Delightedly, the catalytic activity of Pt/PCN-224(Zn) is well retained even

Scheme 2. Proposed Mechanism for the $^1O_2$ Generation and Electron Transfer between Pt and PCN-224(M) in the Oxidation of Benzyl Alcohol over Pt/PCN-224(M) under Visible-Light Irradiation[a]

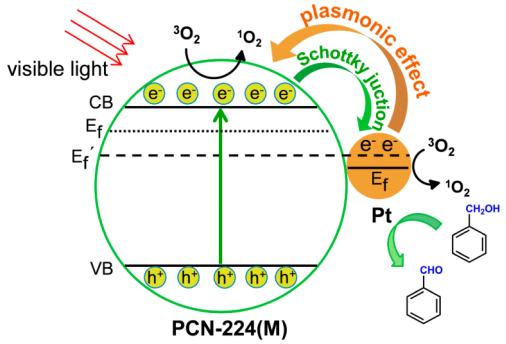

[a]VB, valence band; CB, conduction band; E_f represents the Fermi level of PCN-224(M) or Pt NCs; E_f' represents the Fermi level of Pt/PCN-224(M) composite.

DOI: 10.1021/jacs.6b12074
J. Am. Chem. Soc. 2017, 139, 2035−2044

after six runs of benzyl alcohol oxidation without any treatment or activation (Figure 5a). No significant loss of crystallinity for

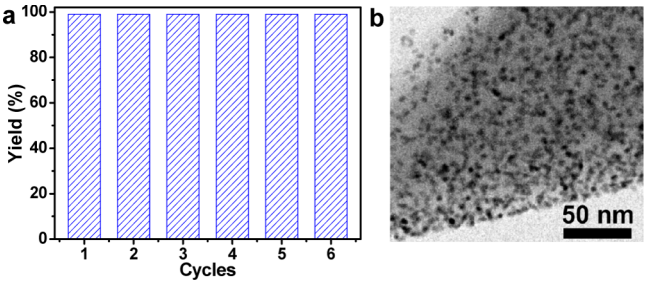

Figure 5. (a) Recyclability of Pt/PCN-224(Zn) in the oxidation of benzyl alcohol. (b) TEM image of Pt/PCN-224(Zn) after catalytic reaction.

PCN-224(Zn) was observed from the PXRD patterns (Figure S21), and aggregation of Pt NCs does not occur from the TEM image after reaction (Figure S5b), suggesting excellent recyclability and stability of Pt/PCN-224(Zn). XPS measurements show that the binding energies of Pt $4f_{5/2}$ and $4f_{7/2}$ remain well before and after reaction, indicating the unchanged oxidation state of Pt during the reaction and excellent stability of Pt/PCN-224(Zn) (Figure S22).

Encouraged by the excellent catalytic performance of Pt/PCN-224(Zn) in the oxidation of benzyl alcohol, we proceeded to investigate the scope of this reaction. Diverse substituted benzyl alcohols and heteroaromatic alcohols were completely oxidized with varying reaction time, but quantitative conversion as well as complete selectivity for aldehyde over carboxylic acid or other oxidizing products was obtained in each case (Table 2). The reactions were completed within 60 min with benzyl alcohol (entry 1) and its substitutions with electron-withdrawing groups ($-NO_2$, $-Cl$, $-Br$) (entries 2–4), while it requires at least 120 min for those bearing electron-donating groups ($-CH_3$, $-NH_2$) or furfuryl alcohol (entries 5–7). The 4-methoxybenzyl alcohol is an abnormality here (entry 8). Despite the presence of the electron-donating methoxy group, the reaction rate is not slowed down as compared to benzyl alcohol (entry 1). In addition to the electronic effect, steric hindrance also significantly slows down the reaction (entries 4, 9, and 10). In the absence of steric hindrance, the 1,4-benzenedimethanol can be quickly converted (entry 11) with a similar catalytic efficiency to that of benzyl alcohol. However, under identical conditions, Pt/PCN-224(Zn) does not present any activity in the oxidation of toluene (entry 12), which generally requires harsh conditions like stronger oxidant or high temperature/pressure.

Table 2. Photo-Oxidation of Various Aromatic Alcohols over Pt/PCN-224(Zn)[a]

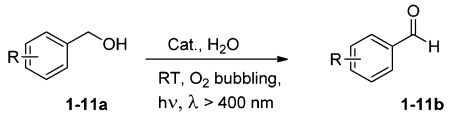

Entry	Substrate	Time (min)	Conversion (%)[b]	Selectivity (%)[b]
1	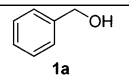 1a	50	>99	100
2	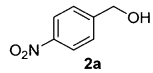 2a	60	>99	100
3	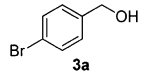 3a	50	>99	100
4	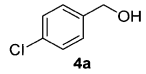 4a	40	>99	100
5	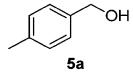 5a	120	>99	100
6	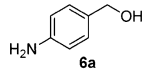 6a	120	>99	100
7	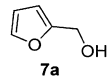 7a	120	>99	100
8	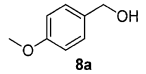 8a	50	>99	100
9	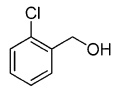 9a	300	>99	100
10	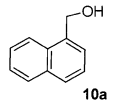 10a	180	>99	100
11[c]	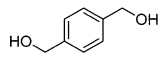 11a	50	>99	100
12	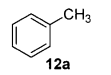 12a	120	-	-

[a]Reaction conditions: catalyst (20 mg, 6.3 μmol Pt), alcohol (20 μmol), 10 mL of H_2O, visible light (λ > 400 nm, 100 mW/cm^2), O_2 (1 atm), starting temperature: 16 °C. [b]Yield of aldehyde was analyzed by GC, and *n*-dodecane was used as the internal standard. [c]Substrate (10 μmol).

CONCLUSIONS

In summary, we demonstrate for the first time the superiority of photochemically generated $^1O_2$ as a mild oxidant for selective oxidation of aromatic alcohols into corresponding aldehydes using Pt/PCN-224(M) as the catalysts. The reactions proceed with excellent selectivity and yield within short reaction time under ambient conditions involving visible-light irradiation. Neither harsh chemicals nor high pressure is needed, and the catalyst can be recycled at least six times without noticeable loss of activity. We carried out detailed studies and found an unusual synergistic effect among the photothermal effect, electronic state of Pt surface, and diamagnetism of metal in the MOF. We attribute the excellent performance of Pt/PCN-224(Zn) composite to the combination of the following factors. (1) Both Pt NCs and PCN-224(Zn) have strong visible-light-harvesting power, and they work synergistically in the composite to achieve an even more pronounced photothermal effect which promotes the oxidation reaction. (2) Under visible-light irradiation, Pt/PCN-224(Zn), synergizing the ability of its individual component for the $^1O_2$ generation, effectively activates O_2 into $^1O_2$, a mild and crucial oxidant for the highly selective oxidation of primary alcohols. (3) Among all PCN-224(M) explored, PCN-224(Zn) exhibits the greatest ability of O_2 activation and $^1O_2$ production due to the strongest

DOI: 10.1021/jacs.6b12074
J. Am. Chem. Soc. 2017, 139, 2035–2044

diamagnetism with the d^{10} configuration of Zn^{2+} among different metals residing in the porphyrin center in the MOF. (4) The electronic state of surface Pt, closely associated with $^1O_2$ generation, can be adjusted flexibly by the competition between a Schottky junction and a plasmonic effect with varying light intensities to achieve optimized O_2 activation. (5) The moderate oxidation ability of $^1O_2$ effectively prevents the overoxidation and thus gives 100% selectivity to aldehyde products. This work represents the first report on the acceleration of catalytic organic oxidations by regulating electronic states of metal surface in metal/MOF composites and their photothermal effect under visible-light irradiation, which will open up a new door to the development of metal/MOF composites, or even metal/semiconductors, for photocatalytic organic reactions.

■ ASSOCIATED CONTENT

Supporting Information

The Supporting Information is available free of charge on the ACS Publications website at DOI: 10.1021/jacs.6b12074.

Additional figures mentioned in the text (PDF)

■ AUTHOR INFORMATION

Corresponding Author

*jianglab@ustc.edu.cn

ORCID

Zhiyong U. Wang: 0000-0003-3701-0862
Hengwei Wang: 0000-0003-1747-4766
Junling Lu: 0000-0002-2607-6869
Shu-Hong Yu: 0000-0003-3732-1011
Hai-Long Jiang: 0000-0002-2975-7977

Notes

The authors declare no competing financial interest.

■ ACKNOWLEDGMENTS

We are grateful to the reviewers for their insightful comments and valuable suggestions. This work was supported by the NSFC (21673213, 21371162, and 21521001), the 973 program (2014CB931803), the Recruitment Program of Global Youth Experts, and the Fundamental Research Funds for the Central Universities (WK2060190065).

■ REFERENCES

(1) Sheldon, R. A.; Arends, I. W. C. E.; ten Brink, G. J.; Dijksman, A. *Acc. Chem. Res.* **2002**, *35*, 774.
(2) Ishida, T.; Nagaoka, M.; Akita, T.; Haruta, M. *Chem. - Eur. J.* **2008**, *14*, 8456.
(3) Karimi, B.; Khorasani, M.; Vali, H.; Vargas, C.; Luque, R. *ACS Catal.* **2015**, *5*, 4189.
(4) Enache, D. I.; Edwards, J. K.; Landon, P.; Solsona-Espriu, B.; Carley, A. F.; Herzing, A. A.; Watanabe, M.; Kiely, C. J.; Knight, D. W.; Hutchings, G. J. *Science* **2006**, *311*, 362.
(5) Sarina, S.; Zhu, H.; Jaatinen, E.; Xiao, Q.; Liu, H.; Jia, J.; Chen, C.; Zhao, J. *J. Am. Chem. Soc.* **2013**, *135*, 5793.
(6) Guo, Z.; Liu, B.; Zhang, Q.; Deng, W.; Wang, Y.; Yang, Y. *Chem. Soc. Rev.* **2014**, *43*, 3480.
(7) Abad, A.; Concepción, P.; Corma, A.; García, H. *Angew. Chem., Int. Ed.* **2005**, *44*, 4066.
(8) Mori, K.; Hara, T.; Mizugaki, T.; Ebitani, K.; Kaneda, K. *J. Am. Chem. Soc.* **2004**, *126*, 10657.
(9) Mallat, T.; Baiker, A. *Chem. Rev.* **2004**, *104*, 3037.
(10) Su, F.; Mathew, S. C.; Lipner, G.; Fu, X.; Antonietti, M.; Blechert, S.; Wang, X. *J. Am. Chem. Soc.* **2010**, *132*, 16299.
(11) Herzberg, G. *Molecular spectra and molecular structure I: spectra of diatomic molecules*, 2nd ed.; VonNostrand: New York, 1950.
(12) Wahlen, J.; De Vos, D. E.; Jacobs, P. A.; Alsters, P. L. *Adv. Synth. Catal.* **2004**, *346*, 152.
(13) Long, R.; Mao, K.; Ye, X.; Yan, W.; Huang, Y.; Wang, J.; Fu, Y.; Wang, X.; Wu, X.; Xie, Y.; Xiong, Y. *J. Am. Chem. Soc.* **2013**, *135*, 3200.
(14) Urakami, H.; Zhang, K.; Vilela, F. *Chem. Commun.* **2013**, *49*, 2353.
(15) Lu, K.; He, C.; Lin, W. *J. Am. Chem. Soc.* **2014**, *136*, 16712.
(16) Park, J.; Feng, D.; Yuan, S.; Zhou, H.-C. *Angew. Chem., Int. Ed.* **2015**, *54*, 430.
(17) Liu, Y.; Howarth, A. J.; Hupp, J. T.; Farha, O. K. *Angew. Chem., Int. Ed.* **2015**, *54*, 9001.
(18) Chen, X.; Addicoat, M.; Jin, E.; Zhai, L.; Xu, H.; Huang, N.; Guo, Z.; Liu, L.; Irle, S.; Jiang, D. *J. Am. Chem. Soc.* **2015**, *137*, 3241.
(19) Ding, X.; Han, B.-H. *Angew. Chem., Int. Ed.* **2015**, *54*, 6536.
(20) Liu, Y.; Moon, S.-Y.; Hupp, J. T.; Farha, O. K. *ACS Nano* **2015**, *9*, 12358.
(21) Wilkinson, F.; Helman, W. P.; Ross, A. B. *J. Phys. Chem. Ref. Data* **1995**, *24*, 663.
(22) DeRosa, M. C.; Crutchley, R. J. *Coord. Chem. Rev.* **2002**, *233–234*, 351.
(23) Montagnon, T.; Tofi, M.; Vassilikogiannakis, G. *Acc. Chem. Res.* **2008**, *41*, 1001.
(24) Kovalev, B. D.; Fujii, M. *Adv. Mater.* **2005**, *17*, 2531.
(25) Ogilby, P. R. *Chem. Soc. Rev.* **2010**, *39*, 3181.
(26) Vankayala, R.; Sagadevan, A.; Vijayaraghavan, P.; Kuo, C.-L.; Hwang, K. C. *Angew. Chem., Int. Ed.* **2011**, *50*, 10640.
(27) Wang, H.; Yang, X.; Shao, W.; Chen, S.; Xie, J.; Zhang, X.; Wang, J.; Xie, Y. *J. Am. Chem. Soc.* **2015**, *137*, 11376.
(28) Long, J. R.; Yaghi, O. M. *Chem. Soc. Rev.* **2009**, *38*, 1213.
(29) Zhou, H.-C.; Long, J. R.; Yaghi, O. M. *Chem. Rev.* **2012**, *112*, 673.
(30) Furukawa, H.; Cordova, K. E.; O'Keeffe, M.; Yaghi, O. M. *Science* **2013**, *341*, 1230444.
(31) Zhou, H.-C.; Kitagawa, S. *Chem. Soc. Rev.* **2014**, *43*, 5415.
(32) Wang, Z. Q.; Cohen, S. M. *Chem. Soc. Rev.* **2009**, *38*, 1315.
(33) Fu, Y.; Sun, D.; Chen, Y.; Huang, R.; Ding, Z.; Fu, X.; Li, Z. *Angew. Chem., Int. Ed.* **2012**, *51*, 3364.
(34) Feng, D.; Chung, W.-C.; Wei, Z.; Gu, Z.-Y.; Jiang, H.-L.; Chen, Y.-P.; Darensbourg, D. J.; Zhou, H.-C. *J. Am. Chem. Soc.* **2013**, *135*, 17105.
(35) Gao, W.-Y.; Chrzanowski, M.; Ma, S. *Chem. Soc. Rev.* **2014**, *43*, 5841.
(36) He, Y.; Zhou, W.; Qian, G.; Chen, B. *Chem. Soc. Rev.* **2014**, *43*, 5657.
(37) Zhao, M.; Ou, S.; Wu, C.-D. *Acc. Chem. Res.* **2014**, *47*, 1199.
(38) Hermes, S.; Schröter, M.-K.; Schmid, R.; Khodeir, L.; Muhler, M.; Tissler, A.; Fischer, R. W.; Fischer, R. A. *Angew. Chem., Int. Ed.* **2005**, *44*, 6237.
(39) Hwang, Y. K.; Hong, D.; Chang, J.-S.; Jhung, S. H.; Seo, Y.-K.; Kim, J.; Vimont, A.; Daturi, M.; Serre, C.; Férey, G. *Angew. Chem., Int. Ed.* **2008**, *47*, 4144.
(40) Jiang, H.-L.; Liu, B.; Akita, T.; Haruta, M.; Sakurai, H.; Xu, Q. *J. Am. Chem. Soc.* **2009**, *131*, 11302.
(41) Yuan, B.; Pan, Y.; Li, Y.; Yin, B.; Jiang, H. *Angew. Chem., Int. Ed.* **2010**, *49*, 4054.
(42) Lu, G.; Li, S.; Guo, Z.; Farha, O. K.; Hauser, B. G.; Qi, X.; Wang, Y.; Wang, X.; Han, S.; Liu, X.; DuChene, J. S.; Zhang, H.; Zhang, Q.; Chen, X.; Ma, J.; Loo, S. C. J.; Wei, W. D.; Yang, Y.; Hupp, J. T.; Huo, F. *Nat. Chem.* **2012**, *4*, 310.
(43) Hermannsdörfer, J.; Friedrich, M.; Miyajima, N.; Albuquerque, R. Q.; Kümmel, S.; Kempe, R. *Angew. Chem., Int. Ed.* **2012**, *51*, 11473.
(44) Dhakshinamoorthy, A.; Garcia, H. *Chem. Soc. Rev.* **2012**, *41*, 5262.
(45) Moon, H. R.; Lim, D. W.; Suh, M. P. *Chem. Soc. Rev.* **2013**, *42*, 1807.

DOI: 10.1021/jacs.6b12074
J. Am. Chem. Soc. 2017, 139, 2035–2044

(46) Khaletskaya, K.; Reboul, J.; Meilikhov, M.; Nakahama, M.; Diring, S.; Tsujimoto, M.; Isoda, S.; Kim, F.; Kamei, K. I.; Fischer, R. A.; Kitagawa, S.; Furukawa, S. *J. Am. Chem. Soc.* **2013**, *135*, 10998.
(47) Hu, P.; Morabito, J. V.; Tsung, C.-K. *ACS Catal.* **2014**, *4*, 4409.
(48) Liu, X.; He, L.; Zheng, J.; Guo, J.; Bi, F.; Ma, X.; Zhao, K.; Liu, Y.; Song, R.; Tang, Z. *Adv. Mater.* **2015**, *27*, 3273.
(49) Yang, Q.; Xu, Q.; Yu, S.-H.; Jiang, H.-L. *Angew. Chem., Int. Ed.* **2016**, *55*, 3685.
(50) Li, Z.; Yu, R.; Huang, J.; Shi, Y.; Zhang, D.; Zhong, X.; Wang, D.; Wu, Y.; Li, Y. *Nat. Commun.* **2015**, *6*, 8248.
(51) Wang, D.; Wang, M.; Li, Z. *ACS Catal.* **2015**, *5*, 6852.
(52) Deenadayalan, M. S.; Sharma, N.; Verma, P. K.; Nagaraja, C. M. *Inorg. Chem.* **2016**, *55*, 5320.
(53) Shiraishi, Y.; Sugano, Y.; Tanaka, S.; Hirai, T. *Angew. Chem., Int. Ed.* **2010**, *49*, 1656.
(54) Chiu, C.-Y.; Yao, Z.; Zhou, F.; Zhang, H.; Ozolins, V.; Huang, Y. *J. Am. Chem. Soc.* **2013**, *135*, 15489.
(55) Jain, P. K.; Huang, X.; El-Sayed, I. H.; El-Sayed, M. A. *Acc. Chem. Res.* **2008**, *41*, 1578.
(56) Wang, F.; Li, C.; Chen, H.; Jiang, R.; Sun, L. D.; Li, Q.; Wang, J.; Yu, J. C.; Yan, C. H. *J. Am. Chem. Soc.* **2013**, *135*, 5588.
(57) Linic, S.; Aslam, U.; Boerigter, C.; Morabito, M. *Nat. Mater.* **2015**, *14*, 567−576.
(58) Song, S.; Wang, X.; Li, S.; Wang, Z.; Zhu, Q.; Zhang, H. *Chem. Sci.* **2015**, *6*, 6420.
(59) Zhai, W.; Xue, S.; Zhu, A.; Luo, Y.; Tian, Y. *ChemCatChem* **2011**, *3*, 127.
(60) Kim, J.; Monllor-Satoca, D.; Choi, W. *Energy Environ. Sci.* **2012**, *5*, 7647.
(61) Yang, J.; Wang, D.; Han, H.; Li, C. *Acc. Chem. Res.* **2013**, *46*, 1900.
(62) Long, R.; Mao, K.; Gong, M.; Zhou, S.; Hu, J.; Zhi, M.; You, Y.; Bai, S.; Jiang, J.; Zhang, Q.; Wu, X.; Xiong, Y. *Angew. Chem., Int. Ed.* **2014**, *53*, 3205.
(63) Sakamoto, H.; Ohara, T.; Yasumoto, N.; Shiraishi, Y.; Ichikawa, S.; Tanaka, S.; Hirai, T. *J. Am. Chem. Soc.* **2015**, *137*, 9324.
(64) Venna, S. R.; Jasinski, J. B.; Carreon, M. A. *J. Am. Chem. Soc.* **2010**, *132*, 18030.
(65) Song, H.; Kim, F.; Connor, S.; Somorjai, G. A.; Yang, P. *J. Phys. Chem. B* **2005**, *109*, 188.
(66) Li, B.; Long, R.; Zhong, X.; Bai, Y.; Zhu, Z.; Zhang, X.; Zhi, M.; He, J.; Wang, C.; Li, Z.-Y.; Xiong, Y. *Small* **2012**, *8*, 1710.
(67) Gomes, A.; Fernandes, E.; Lima, J. L. *J. Biochem. Biophys. Methods* **2005**, *65*, 45.
(68) Gollmer, A.; Arnbjerg, J.; Blaikie, F. H.; Pedersen, B. W.; Breitenbach, T.; Daasbjerg, K.; Glasius, M.; Ogilby, P. R. *Photochem. Photobiol.* **2011**, *87*, 671.
(69) Zhang, K.; Kopetzki, D.; Seeberger, P. H.; Antonietti, M.; Vilela, F. *Angew. Chem., Int. Ed.* **2013**, *52*, 1432.
(70) Josephy, P. D.; Eling, T.; Mason, R. P. *J. Biol. Chem.* **1982**, *257*, 3669.
(71) Badwey, J. A.; Karnovsky, M. L. *Annu. Rev. Biochem.* **1980**, *49*, 695.
(72) Konaka, R.; Kasahara, E.; Dunlap, W. C.; Yamamoto, Y.; Chien, K. C.; Inoue, M. *Free Radical Biol. Med.* **1999**, *27*, 294.
(73) Noda, Y.; Anzai, K.; Mori, A.; Kohno, M.; Shinmei, M.; Packer, L. *IUBMB Life* **1997**, *42*, 35.

DOI: 10.1021/jacs.6b12074
J. Am. Chem. Soc. 2017, 139, 2035−2044